

AFRL-VS-TR-1999-1514

REGIONAL SEISMIC WAVEFIELD CALIBRATION

R. B. Herrmann, M. Raoof, L. Malagnini, M. Samiezade-Yazd, W. Liu

Department of Earth and Atmospheric Sciences
St. Louis University
3507 Laclede Avenue
St. Louis, MO 63103

15 December 1998

Final Report
12 June 1995 - 11 June 1997

Approved for public release; distribution unlimited



**DEPARTMENT OF ENERGY
Office of Non-Proliferation
and National Security
WASHINGTON, DC 20585**

20000920 059



**AIR FORCE RESEARCH LABORATORY
Space Vehicles Directorate
AIR FORCE MATERIEL COMMAND
HANSCOM AIR FORCE BASE, MA 01731-3010**

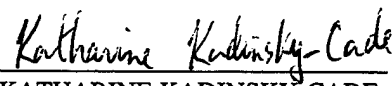
DTIC QUALITY INSPECTED 4

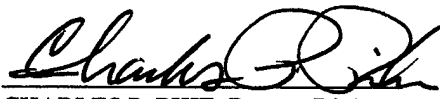
SPONSORED BY
Department of Energy
Office of Non-Proliferation and National Security

MONITORED BY
Air Force Research Laboratory
CONTRACT No. F19628-95-K-0005

The views and conclusions contained in this document are those of the authors and should not be interpreted as representing the official policies, either express or implied, of the Air Force or U.S. Government.

This technical report has been reviewed and is approved for publication.


KATHARINE KADINSKY-CADE
Contract Manager


CHARLES P. PIKE, Deputy Director
Integration and Operations Division

This report has been reviewed by the ESD Public Affairs Office (PA) and is releasable to the National Technical Information Service (NTIS).

Qualified requestors may obtain copies from the Defense Technical Information Center. All others should apply to the National Technical Information Service.

If your address has changed, or you wish to be removed from the mailing list, or if the addressee is no longer employed by your organization, please notify AFRL/VSIP, 29 Randolph Road, Hanscom AFB, MA 01731-3010. This will assist us in maintaining a current mailing list.

Do not return copies of the report unless contractual obligations or notices on a specific document requires that it be returned.

REPORT DOCUMENTATION PAGE

Form Approved
OMB No. 0704-0188

Public reporting burden for this collection of information is estimated to average 1 hour per response, including the time for reviewing instructions, searching existing data sources, gathering and maintaining the data needed, and completing and reviewing the collection of information. Send comments regarding this burden estimate or any other aspect of this collection of information, including suggestions for reducing this burden, to Washington Headquarters Services, Directorate for Information Operations and Reports, 1215 Jefferson Davis Highway, Suite 1204, Arlington, VA 22202-4302, and to the Office of Management and Budget, Paperwork Reduction Project (0704-0188), Washington, DC 20503.

1. AGENCY USE ONLY (Leave blank)

2. REPORT DATE

15 DEC 1998

3. REPORT TYPE AND DATES COVERED

Final Report 12 1995 - 11 1997

4. TITLE AND SUBTITLE

Regional Seismic Wavefield Calibration

5. FUNDING NUMBERS

F19628-95-K-0005

6. AUTHOR(S)

R.B. Herrmann, M. Raoof, ~~E.~~ Malagnini, M. Samiezade-Yazd
and W. Liu

PE 69120H

PR DENN

TA GM

WW AN

7. PERFORMING ORGANIZATION NAME(S) AND ADDRESS(ES)

Department of Earth and Atmospheric Sciences
Saint Louis University
3507 Laclede Avenue
St. Louis MO 63103

8. PERFORMING ORGANIZATION
REPORT NUMBER

9. SPONSORING/MONITORING AGENCY NAME(S) AND ADDRESS(ES)

Air Force Research Laboratory
29 Randolph Road
Hanscom AFB, MA 01731-3010
Contract Manager: Katharine Kadinsky-Cade/VSBS

10. SPONSORING/MONITORING
AGENCY REPORT NUMBER

AFRL-VS-TR-1999-1514

11. SUPPLEMENTARY NOTES

This research was sponsored by the Department of Energy, Office of Non-Proliferation and National Security, Washington, DC 20585

12a. DISTRIBUTION/AVAILABILITY STATEMENT

Approved for Public Release, Distribution Unlimited

12b. DISTRIBUTION CODE

13. ABSTRACT (Maximum 200 words)

This report presents an application of techniques developed to characterize Lg- and S-wave propagation as a function of distance and frequency. We have applied this technique to various regions in the United States and Europe.

14. SUBJECT TERMS

Lg, S-wave, regional wave propagation, seismology

15. NUMBER OF PAGES

44

16. PRICE CODE

17. SECURITY CLASSIFICATION
OF REPORT

Unclassified

18. SECURITY CLASSIFICATION
OF THIS PAGE

Unclassified

19. SECURITY CLASSIFICATION
OF ABSTRACT

Unclassified

20. LIMITATION OF ABSTRACT

SAR

TABLE OF CONTENTS

SECTION	PAGE
Summary	1
1. Introduction	2
2. Data Set	3
3. Duration	4
4. Ground Motion Regression	7
5. Ground Motion Parameterization	10
6. Conclusions	13
7. References	15

Summary

This report presents an application of techniques developed under this contract to use regional seismic network data to define the variation of Lg amplitude with distance and frequency.

The distinguishing feature of this work is that we do not use a simple relation for Lg- or S-wave amplitude variation. Rather we use a very general form

$$a(f, r) = g(r)e(f)s(f)e^{-\pi f r / Q(f)U},$$

where the geometrical term $g(r)$ is not a simple functional relation such as $r - n$. To permit the observed data themselves to define the empirical form, typically 1000 - 2000 wave forms are used in the distance range of interest. Regression is used to define a distance dependence which is then interpreted in a second stage in terms of geometrical spreading and Q . It is at the second stage that a prediction model is developed using random vibration theory as a tool that connects Fourier spectra and signal duration to peak time-domain amplitudes.

The surprising feature that we have noticed in analyzing data from the southern Great Basin surrounding NTS, southern California, the Pacific Northwest, the central United States, Germany and Italy, is the difference in the $g(r)$ at distances greater than 40 km from the source in addition to the expected differences of $Q(f)$. These variations must be the result of regional differences in crustal structure. Our data depend on the structure but are insufficient to define the structure.

The techniques used here are applicable to those parts of the world with regional seismic network observations of local events. While this constraint precludes the universal use of our techniques, they are useful in some regions of interest.

1. Introduction

Ground motion attenuation with distance and the variation of excitation with magnitude are parameterized using three-component, 0.25-5.0 Hz earthquake ground motions in the distance range of 15 - 500 km for southern California. The data set consists of 820 three-component TERRAscope recordings from 140 earthquakes, recorded at 17 stations, with moment magnitudes between 3.1 and 6.7. Regression analysis uses a simple model to relate the logarithm of measured ground motion to excitation, site, and propagation effects. Regression is performed on Fourier velocity spectra and peak velocities in selected narrow band pass filtered frequency ranges. Regression results for Fourier amplitude spectra and peak velocities are used to define a piecewise continuous geometrical spreading function, frequency dependent $Q(f)$, and a distance dependent duration that can be used with random vibration theory (RVT) or stochastic simulations to predict other characteristics of the ground motion.

The duration results indicate that station terms are required and that both the degree of distance dependence and scatter decrease with increasing frequency. The ratio of horizontal to vertical component site terms is about $\sqrt{2}$ for all frequencies. However, this ratio is nearer to unity for rock sites and higher for soil sites.

Modeling indicates that the Fourier velocity spectra are best fit by bilinear geometrical spreading exponents of -1 for $r < 40$ km and $-1/2$ for $r > 40$ km. The frequency dependent quality factor is $Q(f) = 180 f^{0.45}$ for each of the three components and also for the combined three-component data sets. The $T_{5-75\%}$ duration window provides good agreement between observed and RVT predicted peak values.

Estimation of expected ground motion as a function of distance and earthquake magnitude is fundamental to earthquake hazard assessment. The general problem can be stated as follows: given an earthquake at one location, what is the expected ground motion at other locations? Proper design of earthquake-resistant structures and facilities requires estimation of the ground shaking, typically in the 0.2 - 10 Hz frequency band. In addition, inelastic dynamic analysis of structures requires an estimate of signal duration.

Ground motion at a particular site is influenced by three main elements: source, travel path, and local site conditions. Source factors include size, depth, stress drop, rupture process and fault geometry. Travel path factors include geometrical attenuation, dissipation of seismic energy due to anelastic properties of the earth, and focusing and scattering of elastic waves by the three-dimensional earth. Local site factors include the properties of the

uppermost several hundred meters of rock and soil and the effect of the surface topography near the recording site.

The study of ground motion attenuation is also useful for the inverse process of using ground motion recordings to estimate earthquake source parameters, such as magnitude or seismic moment.

Predictive relationships for parameters that decrease with increasing distance (such as peak acceleration and peak velocity) are often referred to as attenuation relationships. A number of attenuation relationships have been proposed for western and eastern North America in the past two decades (Joyner and Boore, 1981; Boore and Joyner, 1991; Boore, 1983; Toro and McGuire, 1987; Atkinson and Boore, 1995; Atkinson and Silva, 1997; Campbell, 1981; Campbell, 1985; Campbell, 1997; and Sadigh 1997). For a given region these relationships may differ because of the nature of the data sets, e.g. three-component accelerograms or regional seismic network data.

The objective of this study is to characterize ground motion observations in Southern California from the TERRAscope network in a manner consistent with random vibration theory (Boore, 1983), which requires signal duration and amplitude spectra to estimate peak motions. Thus, we will examine the variation of Fourier amplitude spectra with distance to specify a geometrical spreading function and a frequency dependent Q operator, and will combine these with a distance and frequency dependent duration function to match peak time domain observations.

2. Data Set

We used TERRAscope seismograms from the IRIS Data Management Center to characterize distance scaling of three-component, 0.25-5.0 Hz earthquake ground motions in the distance range of 15-500 km for southern California. The data set consists of 820 three-component recordings from 140 earthquakes, recorded at 17 stations, with moment magnitudes between 3.1 and 6.7. The maximum frequency of 5-Hz was constrained by the 20 samples/sec sampling rate of the broad-band TERRAscope data.

Figure 1 shows the TERRAscope stations and earthquakes used in this study. Table 1 gives the station coordinates and a description of the site geology as obtained from the FDSN station book. The data set used was chosen to have good overlapping distance sampling by stations (Figure 2), good magnitude coverage (Figure 3), and independently estimated moment magnitudes (Thio and Kanamori, 1995). The TERRAscope data set was used because of its broad band, the broad regional coverage, the large number of observations and easy accessibility. The broadband channels used have a velocity sensitivity that is flat to ground velocity in the 0.25 - 5.0 Hz band.

Table 1
TERRAscope Station Locations and Geology

Stations	Latitude	Longitude	Site Type
BAR	32.680N	116.672W	ROCK, Mesozoic granitic
CALB	34.143N	118.627W	
DGR	33.650N	117.009W	ROCK, Jurassic metamorphic
GLA	33.052N	114.827W	
GSC	35.303N	116.808W	ROCK, Mesozoic granitic
ISA	35.663N	118.473W	ROCK, Mesozoic granitic
MLAC	37.631N	118.834W	SOIL, Quaternary alluvium
NEE	34.823N	114.596W	SOIL, Quaternary alluvium
PAS	34.148N	118.172W	ROCK, Cretaceous quartz diorite
PFO	33.609N	116.455W	ROCK, Cretaceous granodiorite, decomposed
RPV	33.744N	118.404W	SOIL, Quaternary sedimentary rock, sand, rubble
SBC	34.412N	119.713W	SOIL, Quaternary alluvium, sand and gravel
SMTc	32.949N	115.720W	
SNCC	33.248N	119.524W	SOIL, Quaternary alluvium, sand and gravel
SVD	34.104N	117.097W	
USC	34.021N	118.287W	SOIL, Quaternary alluvium
VTV	34.567N	117.333W	SOIL, Quaternary alluvium, gravel, sand and silt

Soil/rock type from station information pages at IRIS where defined.

Time histories were obtained from the IRIS Data Management Center, corrected for instrument response to yield ground velocity in *m/s*. The horizontal components were rotated into radial and transverse components. The corrected time history was then passed through a program that filtered the time series, determined the signal duration, Fourier amplitude spectrum, and peak motion. Filtering involved passing the time history through an 8-pole high-pass followed by an 8-pole low-pass causal Butterworth filter with corner frequencies of $0.707 f_n$ and $1.414 f_n$, where the f_n 's are 0.25, 0.33, 0.4, 0.5, 1, 2, 3, 4, and 5 Hz. Both Fourier spectra and peak time domain values are used in the regression since we desire a self-consistent model linking the three observables.

3. Duration

The duration of ground motion can have a strong influence on earthquake damage. A motion of short duration may not produce enough load reversals for damaging response to build up in a structure, even if the amplitude of the motion is high. On the other hand, a motion with moderate amplitude but long duration can produce enough load reversals to cause substantial damage (Kramer, 1996).

To estimate signal duration, integrated square filtered velocity is used. Other measures of duration have been defined (Kramer, 1996), but we wish to use one consistent with random vibration theory. Integration starts at the S-arrival time and continues into the coda. The duration is defined as the

window within which the integral reached 5% to 75% of its maximum. This is illustrated in Figure 4. The signal duration is a function of the filter center frequency as well as the underlying signal. We encountered some difficulties for low frequencies because of microseism noise, which introduced a linear trend to the integral at large time. This was handled by examining the coda level at the end of the waveform segment to limit the integration window. We also noted increasing scatter as the filter frequencies decreased below 1.0 Hz.

The signal within these 5% and 75% limits was Fourier transformed and RMS averaged between the filter corners to yield the Fourier velocity spectra in m . The peak velocity value of the filtered time history following the S-arrival time was also saved. The data set thus consists of observations of duration, Fourier velocity spectra and peak values of filtered velocities.

A consistent definition of duration is required because an objective of the study is to have a set of observations that permits the use of random vibration theory as described by Boore (1983) who used the work of Cartwright and Longuet-Higgins (CLH) (1956) to relate Fourier spectra to peak motions through signal duration. Equation 6.3 of CLH and its approximations relate expected peak motion to RMS estimates by

$$A_{peak} = \overline{\eta_{max}} A_{RMS}, \quad (1)$$

where A_{RMS} is estimated using Parseval's theorem and the filtered Fourier spectrum within the duration window, $\overline{\eta_{max}}$ is defined by

$$\overline{\eta_{max}} = \int_{-\infty}^{+\infty} \eta \frac{d}{d\eta} [1 - q(\eta)]^N d\eta. \quad (2)$$

Here N is the number of maxima to be exceeded, and $q(\eta)$ is the cumulative probability of η exceeding a given value (CLH 5.1). $p(\eta)$ (CLH 1.19) is a function of the spectral moments; and the number of peaks, N , depends on the moments and signal duration. Equation 6.2 of CLH, for the probability density function of the distribution of peaks,

$$p(\eta_{max}) = \frac{d}{d\eta_{max}} [1 - q(\eta_{max})]^N, \quad (3)$$

is used to examine the probability of not exceeding a peak value by providing confidence bounds on η_{max} .

Figure 5 compares the ratio of observed to predicted time domain peak values at each filter frequency. For each observation the Fourier velocity spectra for the time window is used with the duration to estimate the most likely peak value (Equation 2). In addition the 5% and 95% bounds of the cumulative distribution of peaks are estimated for the peak using Equation 3. Figure 5 aggregates the observations according to these bounds. If random vibration theory is appropriate and if the duration is properly defined, then 90% of the observations should be in the second bin. For example, at 2.00 Hz,

2033 of the 2247 observations are in the second bin. Significant deviations are seen at the low and high filter frequencies for data with low values of peak motion. Of more significance is the observation that the geometric mean of the ratio of observed to predicted peak motions is 0.97. When we used a longer duration based on the 5% - 95% integral signal squared, this ratio differed significantly from 1.0. Because of this exercise, we feel that we have an internally consistent data set of a duration window, Fourier amplitude spectra and peak motions.

Since other studies (Atkinson and Boore, 1995) support a distance-dependent duration, we used a regression model consisting of station terms and piecewise linear segments for the distance dependence, constrained to be zero at zero distance and to be smooth. Station terms were necessary to account for the variability of durations at low filter frequencies. We found significant frequency dependence in the quality of the duration data set and trends. Figures 6 and 7 show the raw three-component duration data for the 0.25 Hz and 1.00 Hz filter frequencies as well as the residuals based on the model. The low frequency duration data exhibit much scatter up to 0.5 Hz. In addition, the station residuals show interesting patterns.

Table 2 presents the station terms at frequencies of 0.25 Hz and 1.0 Hz. To perform the regression, the station correction at Goldstone (GSC) was constrained to be zero. The *Sigma* value is the standard error of the mean *Station Term* and not an indication of distribution of residuals themselves. For stations with more than 90 observations, we note for example, that Santa Barbara (SBC) has a longer duration than Pasadena (PAS) at 0.25 Hz. The variability in station terms may be an artifact of the effect of microseism noise on the automatic determination, but may also be real, reflecting reverberation of these low frequency waves caused by local, perhaps shallow, 3-D structure. The standard error of fit of 53.5 sec is high for the 0.25 Hz data, perhaps because no data screening was performed. Figure 6 seems to show a tendency for the scatter in residuals to increase with distance. The regression model of station terms plus a distance effect may be inappropriate in the sense that the station terms are assumed independent of distance.

The conclusion is that station terms are required and that both the degree of distance dependence and scatter decrease with increasing frequency. In a comparison of durations at all filter frequencies, Figure 8 shows that the low frequency signal components have longer durations than high frequency components. The durations at different distances for different frequencies are listed on Table 3.

Table 2
Station Residuals from Duration Regression Analysis

Station	Station Term	Sigma	NOBS
0.25 Hz Variance Reduction 17.5% σ 53.5 sec			
BAR	25.3	10.8	31
CALB	24.7	11.9	21
DGR	70.4	15.5	13
GLA	29.5	20.9	7
GSC	0.0	0.0	119
ISA	18.1	6.4	129
MLAC	8.6	12.6	21
PAS	25.3	5.2	178
PFO	24.5	5.5	133
RPV	61.3	8.8	43
SBC	59.7	6.9	94
SNCC	0.1	31.5	3
SMTC	63.9	19.1	9
SVD	18.3	7.8	58
USC	57.3	9.1	39
VTV	12.3	8.5	48

1.00 Hz Variance Reduction 53.5% σ 6.7 sec

BAR	3.9	1.0	59
CALB	9.8	1.0	46
DGR	2.1	1.8	15
GLA	-3.6	2.0	12
GSC	0.0	0.0	234
ISA	-1.1	0.6	281
MLAC	7.4	1.2	37
NEE	21.8	1.4	24
PAS	0.0	0.5	333
PFO	3.8	0.6	255
RPV	8.3	0.8	79
SBC	11.7	0.7	174
SNCC	16.1	2.7	6
SMTC	41.5	2.1	12
SVD	2.4	0.7	113
USC	17.1	0.8	77
VTV	0.6	0.8	86

4. Ground Motion Regression

The regression analysis for peak motion and Fourier velocity spectra uses the same simple model. Assuming a multiplicative effect of source, propagation, and site, the logarithm of the ground motion parameter is modeled as the separable effects of source, site, and propagation:

Table 3

Distance (km)	Durations for different Frequencies (Hz)								
	0.25	0.33	0.4	0.5	1.0	2.0	3.0	4.0	5.0
0	0	0	0	0	0	0	0	0	0
40	12.47	9.81	12.30	13.12	9.16	5.90	4.78	4.09	3.72
80	24.63	19.37	22.80	20.23	11.55	7.86	6.60	5.67	5.04
120	35.75	28.21	28.34	21.01	10.61	8.06	6.64	5.71	5.09
160	45.21	35.99	28.96	21.26	12.33	9.08	7.41	6.36	5.61
200	53.20	42.90	36.39	28.49	14.82	10.96	8.99	7.91	7.11
250	60.10	49.05	37.71	28.62	17.10	13.10	11.09	9.66	8.90
300	66.74	54.92	33.74	24.65	19.20	14.96	13.24	11.31	10.72

$$PEAK = \log A = SRC(f) + SITE(f) + D(r, f) \quad (4)$$

Here $D(r)$ is the propagation term, expressing the combined effect of geometrical spreading and attenuation. While simple in appearance, true separability is impossible because of tradeoffs. Care must be taken to select sites which observe earthquakes at many distances so that observations from sites overlap to avoid an undesirable trade-off between an event source term and the distance function. Constraints must also be applied, such as forcing $D(r) = 0$ at some reference distance, such as $D(r_{ref}) = 0$. The reference distance r_{ref} used is such that errors in source depth make little difference on hypocentral distance and that regional variations in high amplitude Moho reflected signals are avoided. Additionally, some or all of the site terms must be constrained, such as $\sum_{i=0}^n SITE_i = 0$, which has the side effect of forcing common site effects into all source terms. This permits the determination of a relative site response only. Any common site term is mapped into the source term. For this study, this constraint was placed only on the horizontal components - the vertical components were free to move relative to the horizontal. Since the initial computations show that the SITE terms for the horizontal components at GSC were small, we further constrained each of the two horizontal component SITE terms for GSC to be zero.

To emphasize the fact that we are not defining the earthquake source on the basis of our data set, but rather parameterizing the observed motions, equation (4) is rewritten as

$$PEAK = \log A = E(f, r_{ref}) + S(f) + D(r, f), \quad (5)$$

where E represents the excitation of the ground motion at the reference distance and S is the site term. Later we will compare predicted levels of ground motion at the reference distance.

Investigations by Atkinson and Boore (1995) in eastern North America and by Atkinson and Silva (1997) in California, indicate that the distance dependence does not have a simple functional form. However, the geometrical spreading may be expressed as a piecewise continuous linear relation.

Anderson and Lei (1994), Savage (1995) and Harmsen (1997) extended this concept to permit many linear segments to be tied together with a smoothness constraint. This means that definition of geometrical spreading and frequency dependent Q is deferred to a later stage. At a given frequency we model $D(r)$ as a piecewise linear function defined by

$$D(r) = \sum_{i=0}^n L_i(r) D_i, \quad (6)$$

and where $L_i(r)$ is a linear interpolation function, and the D_i are node values such that $D(r_i) = D_i$. A smoothness constraint can be applied by requiring

$$D_{i-1} - 2D_i + D_{i+1} = 0. \quad (7)$$

Minimum roughness is easily incorporated if the nodes at distances r_i are evenly spaced.

In this study, a coda normalization (Aki, 1980 ; Frankel *et al*, 1990) was used to provide an initial estimate of the distance term $D(r)$, by removing the effects of source and site from the logarithm of peak ground motion, A . The initial $D(r)$ was then used in an interactive, damped least-squares regression to estimate excitation, site and distance functions. Alternatively, a high quality data set such as this one could start with $D(r) = \log_{10}(r_{ref}/r)$ as an initial estimate. The distance function is parameterized as a piecewise linear function with 17 nodes between 10 and 500 km.

For our regression, we chose $r_{ref} = 40$ km. For each filter frequency there were 140 event terms, 51 site terms for the 17 three-component stations, and 13 nodes in the distance function. Table 4 gives the number of observations, standard deviation of residuals and standard error of the mean residual for the Fourier and time domain regressions. The mean residual is zero.

Table 4
Regression Error Analysis

f_n (Hz)	Fourier Domain			Time Domain		
	N_{OBS}	σ	σ_μ	N_{OBS}	σ	σ_μ
0.25	2204	0.299	0.006	2204	0.153	0.003
0.33	2284	0.162	0.003	2284	0.155	0.003
0.40	2349	0.115	0.002	2349	0.158	0.003
0.50	2375	0.117	0.002	2375	0.158	0.003
1.00	2408	0.125	0.003	2408	0.164	0.003
2.00	2403	0.135	0.003	2403	0.180	0.004
3.00	2384	0.142	0.003	2384	0.185	0.004
4.00	2354	0.150	0.003	2354	0.187	0.004
5.00	2317	0.161	0.003	2317	0.193	0.004

Figures 9 and 10 show the $D(r)$ functions for the Fourier and time domain data sets, respectively, as a function of frequency. To enhance presentation, these figures show the deviation from a r^{-1} trend. For clarity, error bars are not plotted. Subtle differences are seen at larger distances, which

are interpreted as the effect of duration on the time domain observations. Figures 11 and 12 show the distribution of regression residuals as a function of distance for the two data sets at selected frequencies. This plot is used to check the appropriateness of the distance nodes used to determine $D(r)$ since distance trends would be apparent.

The site terms are similar for the time and frequency domain data sets. Figures 13 and 14 give the site terms for the Fourier velocity spectra data set. In general, the site terms for the radial and transverse components overlay. The horizontal components site terms exceed the vertical terms and the frequency dependence varies from station to station. Because of the constraint applied to the horizontal components site term at GSC, we may interpret the excitation terms of equation (4) as being the horizontal ground motion level for an earthquake 40 km from GSC. This distinction is important if one wishes to relate the excitation and site terms to strong motion data sets, which use data from a different network.

There is much variation in the site terms among the stations shown in Figures 13 and 14. The extremes are bounded by $[-0.7, 0.6]$. The horizontal to vertical ratio is slightly less variable. This logarithmic ratio of horizontal to vertical component site terms, and mean logarithmic ratios for soil, rock, and all site types are shown on Figure 15 and are listed in Table 5, for the Fourier velocity spectra. The site type is that given in Table 1. There is little difference between the estimates for the two domains. The H/Z ratio mean varies for the different site types with a mean value corresponding to about $\sqrt{2}$.

Table 5
Mean Logarithmic Ratio of Horizontal To Vertical Site Terms

f_n (Hz)	Rock	All	Soil
0.25	0.094	0.138	0.236
0.33	0.087	0.131	0.237
0.40	0.089	0.127	0.213
0.50	0.092	0.125	0.195
1.00	0.144	0.171	0.225
2.00	0.183	0.206	0.258
3.00	0.138	0.168	0.237
4.00	0.151	0.169	0.222
5.00	0.180	0.175	0.179

5. Ground Motion Parameterization

The next step in the analysis is to define geometrical spreading and anelastic attenuation functions to describe the Fourier velocity spectra $D(r)$ term. This is done by assuming $Q(f) = Q_0 f^n$ and a simple piecewise linear geometrical spreading function. The functional form $g(r)$ for geometrical

spreading, is

$$g(r) = \begin{cases} r^{-1} & r \leq r_{cross} \\ (r/r_{cross})^{-1/2} & r \geq r_{cross} \end{cases}$$

The effect of anelastic attenuation is to reduce amplitude with distance by a factor of $\exp(-\pi f r / Q(f) \beta)$, where $\beta = 3.5$ km/sec.

For a set of the parameters Q_0 , η and r_{cross} , theoretical Fourier spectra were estimated at each of the distances used in the regression for $D(r)$, the results were normalized to the reference distance of 40 km, and a logarithm taken for direct comparison with the regression results. A search is made through the parameter space to find the minimum of

$$\frac{\sum_i [(D_{i,obs} - D_{i,pred}) / \sigma_i]^2}{\sum_i (1/\sigma_i)^2}$$

The σ_i are those resulting from the regression. As a check we also compared the $D(r)$ values obtained from the time domain regression by making random vibration theory estimates of peak filtered ground velocities using the observed durations and random vibration theory (Boore, 1983). We accounted for the time domain response of the filters in the manner of Boore and Joyner (1984) for lightly damped single degree of freedom oscillators by stating that the RMS duration is the sum of the source duration, propagation duration, and twice the filter period. In addition the duration used for determining the number of random peaks is the sum of the source duration, the propagation duration and the filter period.

This exercise yielded $r_{cross} = 40$ km, $Q_0 = 180$ and $\eta = 0.45$. Figures 16 and 17 present the residuals for the Fourier velocity and time domain $D(r)$ functions, respectively. The comparison shows the values for the distance range of 20 - 500 km, because of the paucity of data in the 10 - 20 km range. The fit of the time domain data is an indication of the appropriateness of the duration function used, when combined with the frequency domain model.

Previous work by Atkinson and Silva (1997) resulted in $Q_0 = 204$, $\eta = 0.56$, and a trilinear geometric spreading function with exponents of -1, 0 and 1/2 for $r \leq 50$ km, $50 \leq r \leq 170$ km, and $r > 170$ km, respectively. A comparison of the difference between our observed Fourier velocity $D(r)$ and that predicted by their values is given in Figure 18. Their data set has relatively few observations beyond 100 km and is dominated by the June 28, 1992, $M_w = 7.3$, at large distances. We have better agreement with the regressions of Harmsen (1987) who used TERRAscope data in the 10 - 150 km range. The relation for $Q(f)$ obtained in our study is more in agreement with the regional attenuation relationship for southern California by Benz *et al.*, (1997), which gives $Q(f) = 187_{-7}^{+7} f^{0.56(\pm 0.03)}$. However, their data set includes both southern and central California for a distance range of $150 < r < 700$ km.

As a final comparison, we compared the observed excitation levels of the horizontal motion for both data sets at 40 km to model-based predictions as a function of moment magnitude. Since there are few data for $M_W > 5.5$, we did not feel confident in defining a source excitation model, which would also have suffered by the extrapolation of our observations to a nominal 1 km distance. Instead we compared our excitation levels at 40 km to that derived from two models in literature, one by Atkinson and Boore (1998) and the other by Boore and Joyner (1997). The model for the horizontal site acceleration spectrum is

$$A(f) = C(2\pi f)^2 M_0 S(f) g(r) \exp(-\pi r / \beta Q(f)) V(f)$$

where

$$C = (0.55)(0.707)(2.0)/4\pi\rho\beta^3,$$

and $V(f)$ is a site amplification term. The functional form for $S(f)$ is

$$S(f) = \frac{1-\varepsilon}{1+(f/f_a)^2} + \frac{\varepsilon}{1+(f/f_b)^2}$$

and the f_a , f_b and ε are given by Atkinson and Boore (1998) and repeated in Table 6.

Table 6
Source Parameters

Atkinson and Boore (1998)	
ρ	2.8
β	3.5
f_a	$\log f_a = 2.181 - 0.496M \quad M \geq 4.8$ $ = 2.617 - 0.500M \quad M \leq 4.8$
f_b	$\log f_b = 1.308 - 0.277M \quad M \geq 4.8$ $ = 2.617 - 0.500M \quad M \leq 4.8$
ε	$\log \varepsilon = 3.223 - 0.670M \quad M \geq 4.8$ $ = 0.0 \quad M \leq 4.8$
Boore and Joyner (1997)	
ρ	2.8
β	3.5
$\Delta\sigma$	70 bars
f_a	$f_a = 4.9 \times 10^6 \beta (\Delta\sigma/M_0)^{1/3}$
f_b	$f_b = f_a$
ε	$\varepsilon = 1.0$

We use propagation durations of 12.5 sec at 0.25 Hz, 9.2 sec at 1.0 Hz, and 3.7 sec at 5 Hz at 40 km. The source duration is $0.5/f_a$. We use a κ of 0.040 sec and 0.035 sec for the Atkinson and Boore (1998) and Boore and Joyner (1997) models, respectively. The $V(f)$ term is taken from Atkinson and Silva (1997) and is based on that in Boore (1986).

Figures 19 and 20 compare the excitations at 40 km from our regressions with the predictions based on the two source models combined with our geometrical spreading, anelastic attenuation and duration functions. To emphasize differences, $E + 8 - M_w$ is plotted. Our results share the trends of the two models as a function of moment magnitude. Both models underpredict low frequency levels at small moments. The Boore and Joyner constant stress drop (1997) model seems to fit the high frequency data better than the Atkinson and Boore (1998) model, but recall that these figures are for expected motions at GSC.

Finally, the results of this study indicate that the modern TERRAscope data set agrees with strong motion measurements in estimating distance dependence, which has been also noted by Harmsen (1997). A direct comparison with strong motion data sets requires a joint inversion of both data sets.

6. Conclusions

Using ground velocities from the three-component recordings of the TERRAscope, we have characterized the ground velocity distance scaling in the range of 15 - 500 km for Southern California. Our ground motion scaling is similar to those of other studies which have used TERRAscope data (Benz *et al.*, 1997; Harmsen, 1997). The major differences of our study are the use of Fourier velocity spectra, signal duration, and peak value of filtered time domain velocities.

The results of this study indicate that low frequency signal components have longer durations than high frequency components and increase significantly with distance. The low frequency duration data exhibit much scatter up to 0.5 Hz. The duration results indicate that station terms are required and that both the degree of distance dependence and scatter increase with decreasing frequency. The variability in the station terms may be due to the effect of microseism noise or due to reverberation of low frequency waves by local 3-D structure. These long durations may be important for assessing the response of structures with low natural frequencies.

The distance functions obtained from the Fourier and time domain data sets are similar in trend. Subtle differences at larger distances can be interpreted as the effect of duration on the time domain observations. The site terms are similar for the time and frequency domain data sets. In general, the site terms for the radial and transverse components are quite similar. The horizontal motions exceed the vertical and the frequency dependence of this ratio varies from station to station. The ratio of horizontal to vertical component site terms is about $\sqrt{2}$ for all frequencies. However, this ratio is close to one for rock sites but higher for soil sites alone. There is much variability in the site terms among stations.

Random Vibration Theory (RVT) has been used to model the observed peak ground motion. Peak velocities are controlled by a combination of duration, geometrical spreading, and anelastic attenuation. The results of RVT application indicate that our data fit well by bilinear geometrical spreading exponents of -1 for $r < 40$ km and -1/2 for $r > 40$ km. The frequency dependent quality factor is $Q(f) = 180 f^{0.45}$ for the combined three-component data sets. Our observations show the effect of duration as a factor relating the Fourier amplitude spectra to the peak amplitude scaling.

The comparison of the excitation at 40 km from our regressions with the predictions based on the two models, one by Atkinson and Boore (1998) and the other by Boore and Joyner (1997), indicate that our results share the trends of the two models as a function of moment magnitude. Both models overpredict high frequency levels. This is due to our use of the $V(f)$ function developed for strong motion sites and the fact that the TERRAscope data set has not been used together with strong motion data in an inversion. Because of the smaller number of large events, we cannot distinguish between the Atkinson and Boore (1998) and the Boore and Joyner (1997) models, even though the Boore and Joyner (1997) model seems slightly better.

A comparison of the Fourier domain excitation terms (Fig. 19) to the time domain terms (Fig. 20) shows the same relative pattern between the data and predictions. This supports the internal consistency of our parameterization of the data in terms of anelastic attenuation, geometrical spreading, and duration, since the time domain values use a duration that increases with moment magnitude.

Finally, the results of this study indicate that the modern TERRAscope data complement strong motion measurements in estimating distance dependence (Figure 18 at distances less than 80 km).

7. References

- Aki, K. (1980). Attenuation of shear waves in the lithosphere for frequencies from 0.05 to 25 Hz, *Phys. Earth Planet. Inter.* **21**, 50-60.
- Anderson, J. G., and Y. Lei (1994). Non parametric Description of Peak Acceleration as a Function of Magnitude, Distance, and Site in Guerrero, Mexico, *Bull. Seism. Soc. Am.*, **84**, 1003-1017.
- Atkinson, G. M., and D. M. Boore (1995). Ground-motion relations for eastern North America, *Bull. Seism. Soc. Am.*, **85**, 17-30.
- Atkinson, G. M., and D. M. Boore (1998). Evaluation of Models for earthquake source spectra in eastern north America, *Bull. Seism. Soc. Am.*, (in review)
- Atkinson, G. M., and W. Silva (1997). An Empirical study of earthquake source spectra for California earthquakes, *Bull. Seism. Soc. Am.*, **87**, 97-113.
- Benz, H. M., A. Frankel, and D. M. Boore (1997). Regional Lg attenuation for the Continental United States, *Bull. Seism. Soc. Am.*, **87**, 606-619.
- Boore, D. M. (1983). Stochastic simulation of high-frequency ground motions based on seismological models of the radiated spectra, *Bull. Seism. Soc. Am.*, **73**, 1865-1894.
- Boore, D. M. (1986). Short-period P- and S-wave radiation from large earthquakes: implications for spectral scaling relations, *Bull. Seism. Soc. Am.* **76**, 43-64.
- Boore, D. M., and W. B. Joyner (1984). A Note on the Use of Random Vibration Theory to predict peak amplitudes of transient signals, *Letter to the Editor, Bull. Seism. Soc. Am.*, **74**, 2035-2039.
- Boore, D. M., and W. B. Joyner (1991). Estimation of ground motion at deep-soil sites in eastern North America, *Bull. Seism. Soc. Am.*, **81**, 2167-2185.
- Boore, D. B., and W. B. Joyner (1997). Site Amplification for generic rock sites, *Bull. Seism. Soc. Am.* **87**, 327-341.
- Campbell, K.W. (1981). Near-source attenuation peak horizontal acceleration, *Bull. Seism. Soc. Am.* **71**, 2039-2070.
- Campbell, K.W. (1985). Strong motion attenuation relation: a ten-year perspective, *Earthquake Spectra*, **1**, 759-804.
- Campbell, K.W. (1997). Empirical near-source attenuation relationships for Horizontal and vertical components of peak ground acceleration, peak velocity, and pseudo-absolute acceleration response spectra *Seism. Res. Lett.*, **68**, No. 1, 154-179.
- Cartwright, D. E. and M. S. Longuet-Higgins (1956). The statistical distribution of the maxima of a random function, *Proc. Roy. Soc. London, Ser. A* **237**, 212-223.
- Frankel, A., A. McGarr, J. Bicknell, J. Mori, L. Seeber and E. Cranswick (1990). Attenuation of high-frequency shear waves in the crust:

- measurements from New York state, South Africa, and southern California, *J. Geophys. Res.* **95**, 17,441-17,457.
- Harmsen, S. (1997). Estimating the Diminution of Shear-Wave Amplitude with Distance: Application to the Los Angeles, California, Urban Area *Bull. Seism. Soc. Am.* **87**, 888-903.
- Joyner, W. B. and D. M. Boore (1981). Peak horizontal acceleration and velocity from strong motion records including records from the 1979 Imperial Valley, California, earthquake, *Bull. Seism. Soc. Am.* **71**, 2011-2038.
- Kramer, S. L. (1996). *Geotechnical Earthquake Engineering*, Prentice Hall.
- Savage, K. S. (1995). A local-magnitude scale for the western Great Basin-Eastern Sierra Nevada from Synthetic Wood-Anderson Seismograms, *Bull. Seism. Soc. Am.* **85**, 1236-1243.
- Sadigh, K. (1997). Attenuation relationships for shallow crustal earthquakes based on California strong motion data, *Seism. Res. Lett.*, **68**, No. 1, 180-189.
- Thio, H. K., and H. Kanamori (1995). Moment tensor inversions for local earthquakes using surface waves recorded at TERRAscope, *Bull. Seism. Soc. Am.* **85**, 1021-1038.
- Toro, G. R. and R. K. McGuire (1987). An investigation into earthquake ground motion characteristics in eastern north America, *Bull. Seism. Soc. Am.* **77**, 468-489.

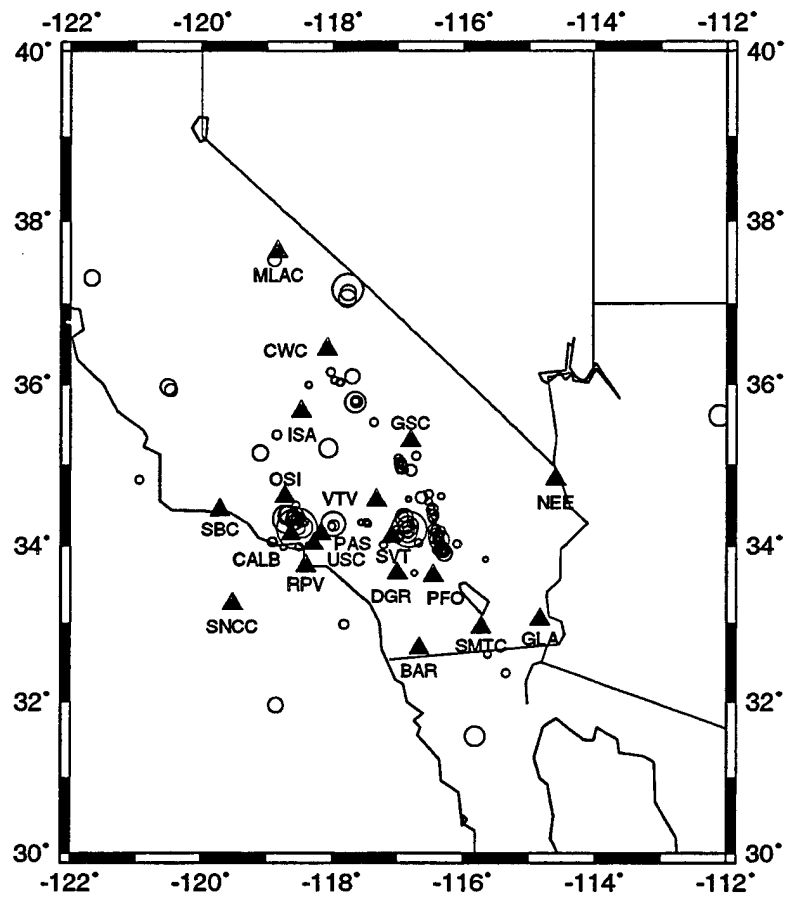


Fig. 1. Locations of TERRAscope stations used (solid triangles) and earthquakes (open circles). The size of the circle is an indication of relative earthquake magnitudes.

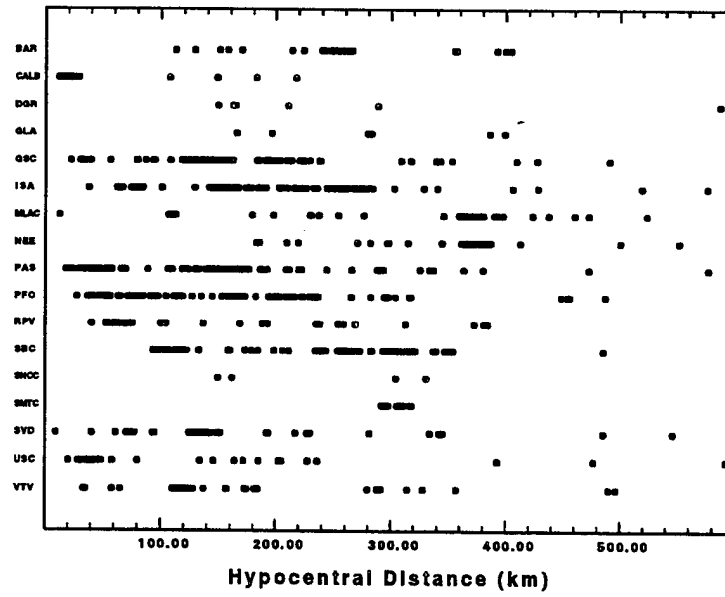


Fig. 2. Distance distribution of data set arranged by station.

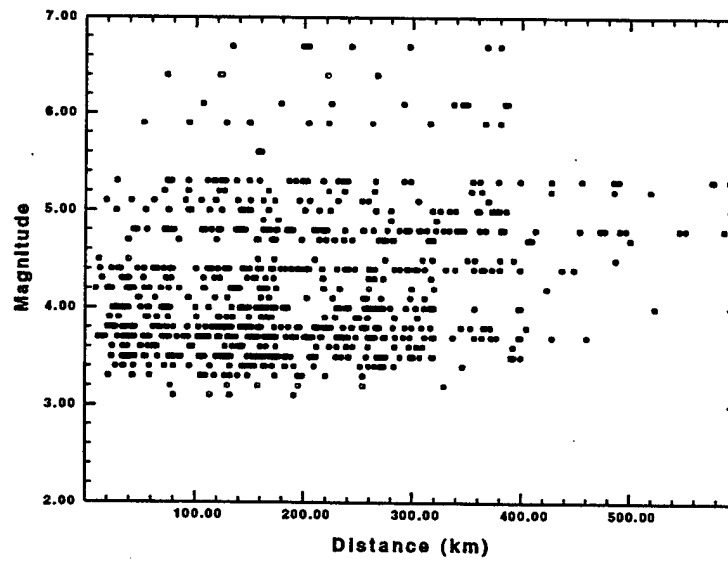


Fig. 3. Distance distribution of data set arranged by moment magnitude.

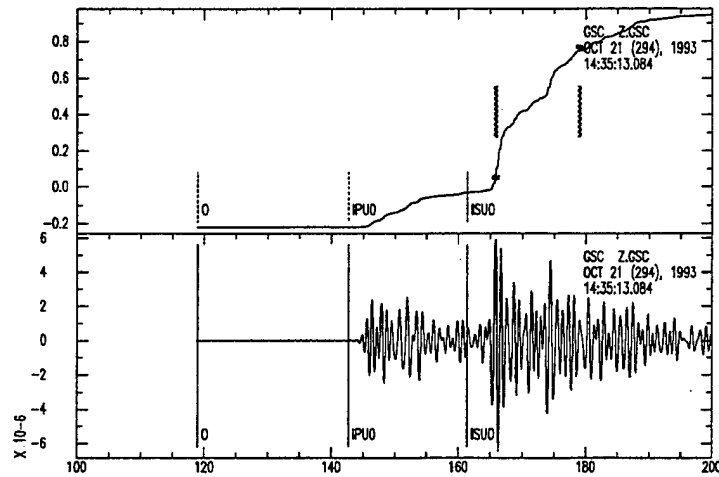


Fig. 4. Illustration of method of estimating duration. The lower trace is the velocity time history filtered at 1.0 Hz. The upper trace is the integrated square velocity. The duration of 14 s is the time interval between the 0.05 and 0.75 ordinate (small squares and heavy vertical bars in upper figure). The origin, P- and S-arrival times (IPU0 and ISU0, respectively) from the unfiltered time history are indicated. The group delay of the filter is apparent by the shift of the P- and S-arrivals from the picked time.

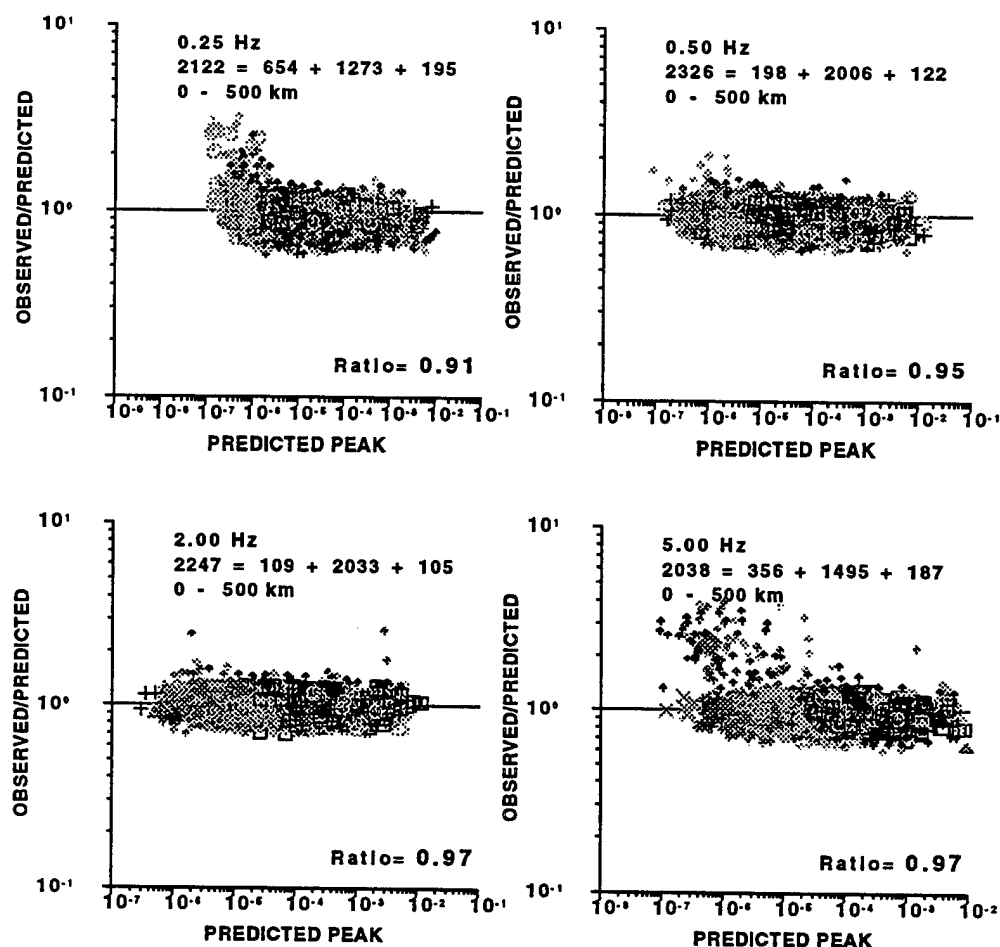


Fig. 5. Comparison of ratio of observed to predicted peak amplitudes as a function of predicted peaks for the entire data set at the different filter frequencies. Each figure indicates the filter frequency, the total number of observations separated as to whether the observed peak was in the 0-5%, 5-95% or in the 95-100% bounds of the predicted peak, the distance range, and the geometric mean ratio.

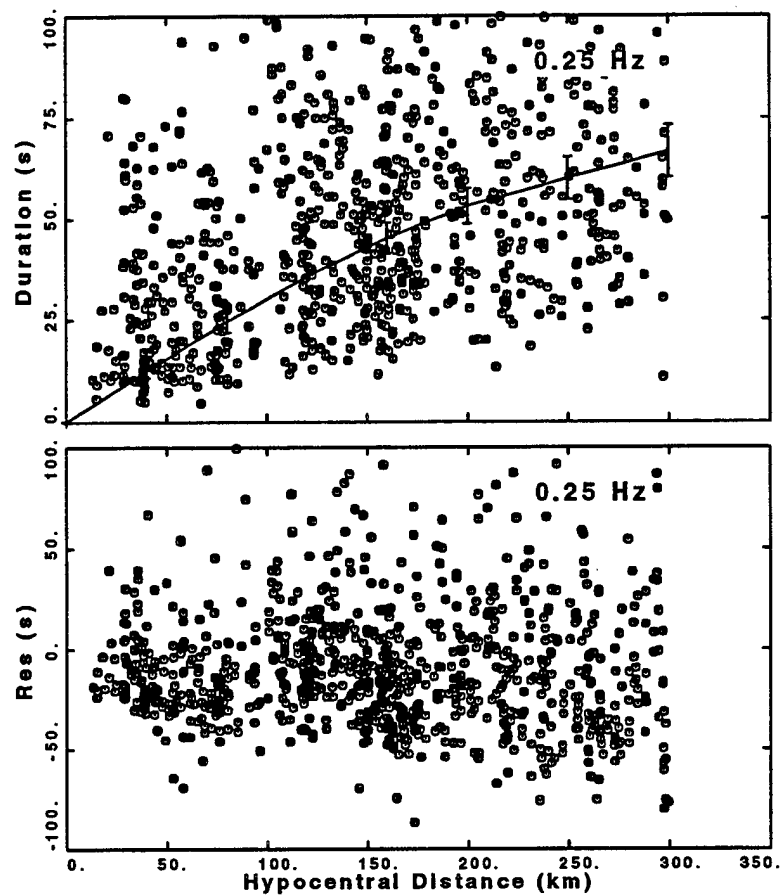


Fig. 6. Duration data and regression line (top) and regression residuals as a function of distance for a filter frequency of 0.25 Hz.

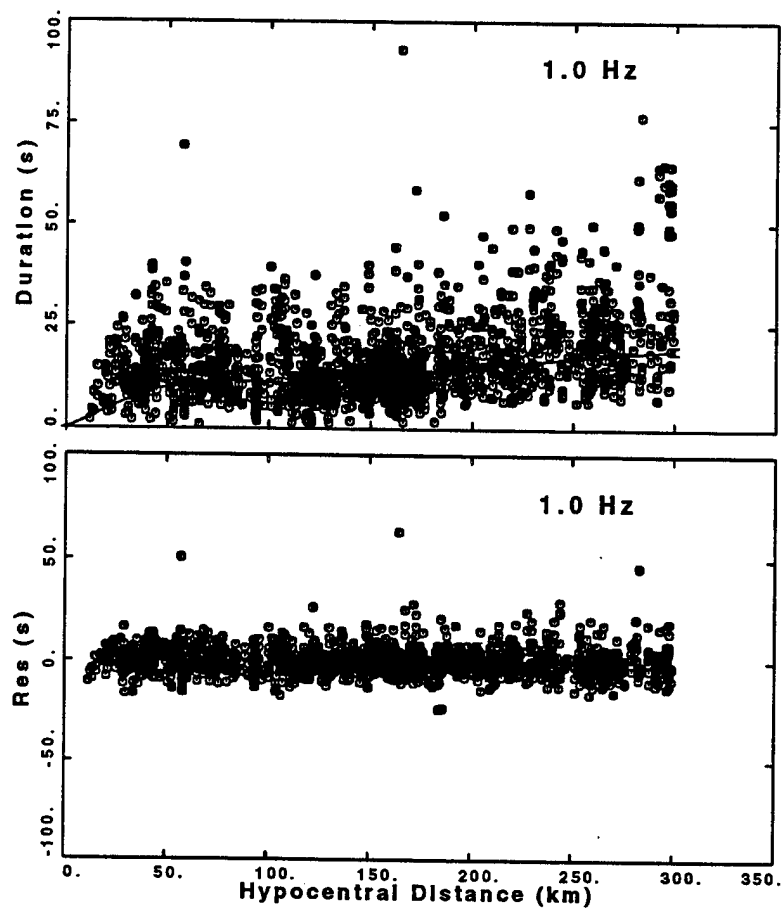


Fig. 7. Duration data and regression line (top) and regression residuals as a function of distance for a filter frequency of 1.00 Hz.

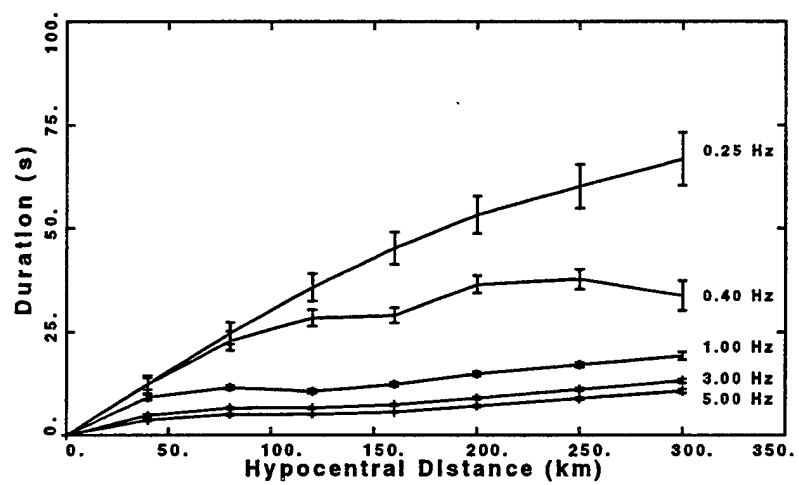


Fig. 8. Distance dependence of duration for 0.25, 0.40, 1.0, 3.0 and 5.0 Hz filtered data.

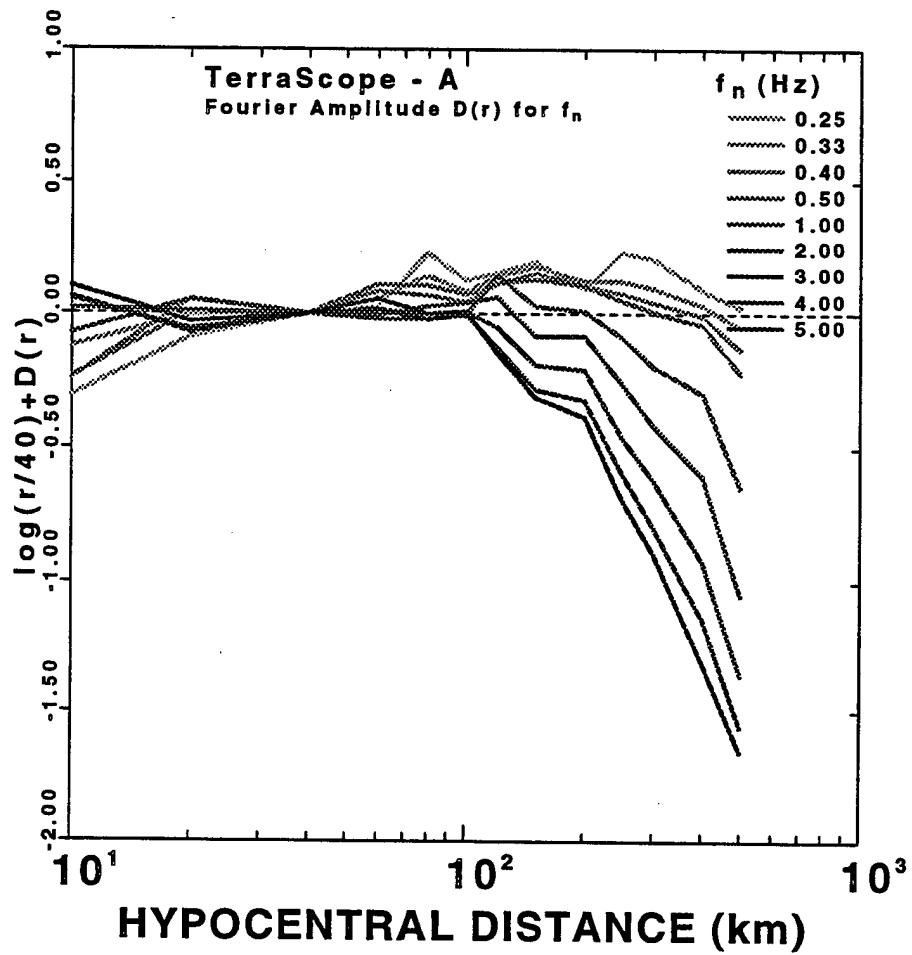


Fig. 9. Frequency dependence of Fourier velocity spectra $D(r)$ corrected for R^{-1} spreading.

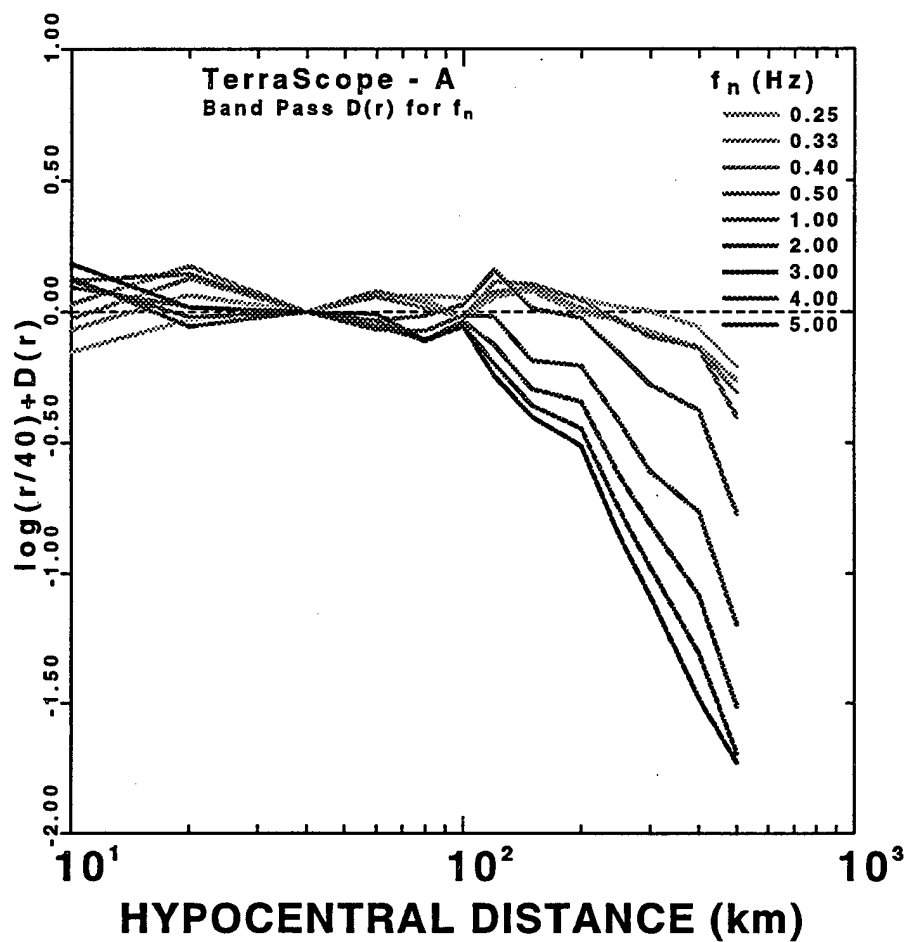


Fig. 10. Frequency dependence of filtered time domain $D(r)$ corrected for R^{-1} spreading.

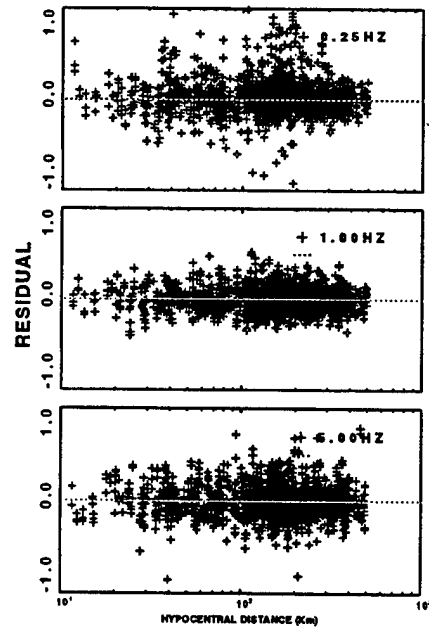


Fig. 11. Distance dependence of regression residuals for Fourier velocity spectra for frequencies of 0.25, 1.0 and 5.0 Hz.

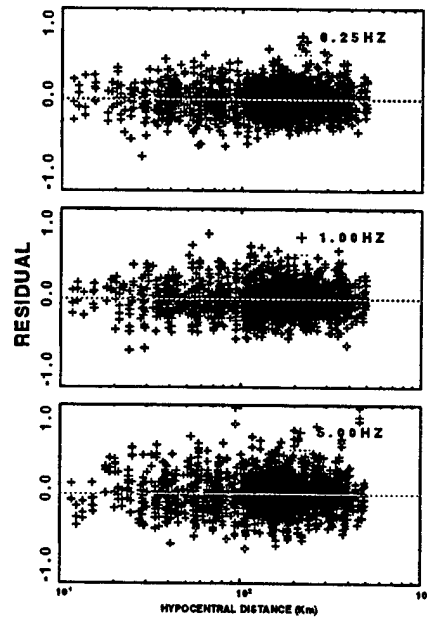


Fig. 12. Distance dependence of regression residuals for peak filtered velocity for frequencies of 0.25, 1.0 and 5.0 Hz.

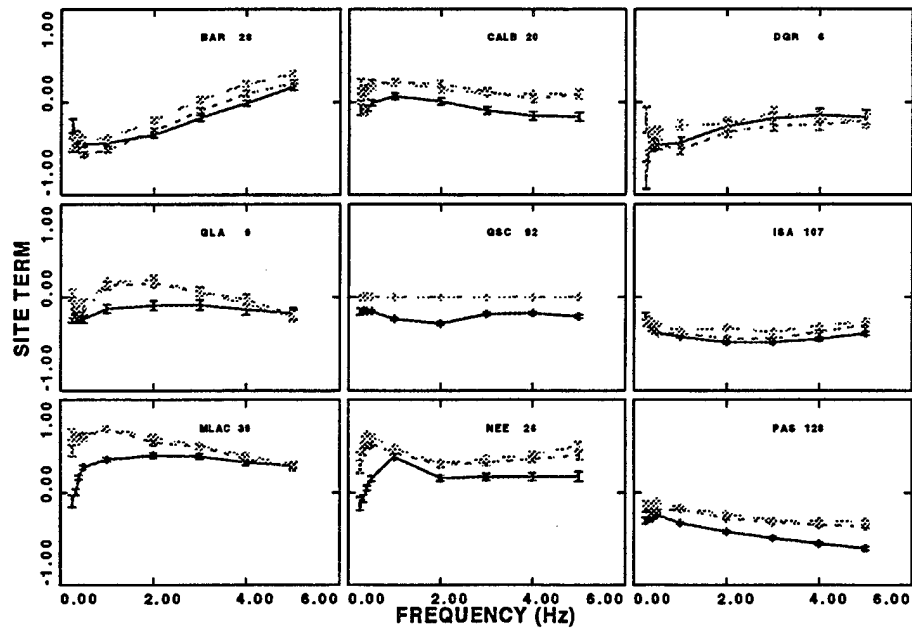


Fig. 13. Site terms for Fourier velocity spectra as a function of frequency. The Z component is indicated by the dark, solid line; the R component is indicated by the medium shade, short-dashed line ; the T component is indicated by the light, long-dashed line. Regression error bars are indicated. Adjacent to the station name is the number of vertical component observations at 1.0Hz; this permits a visual weighting of the importance of any station site term.

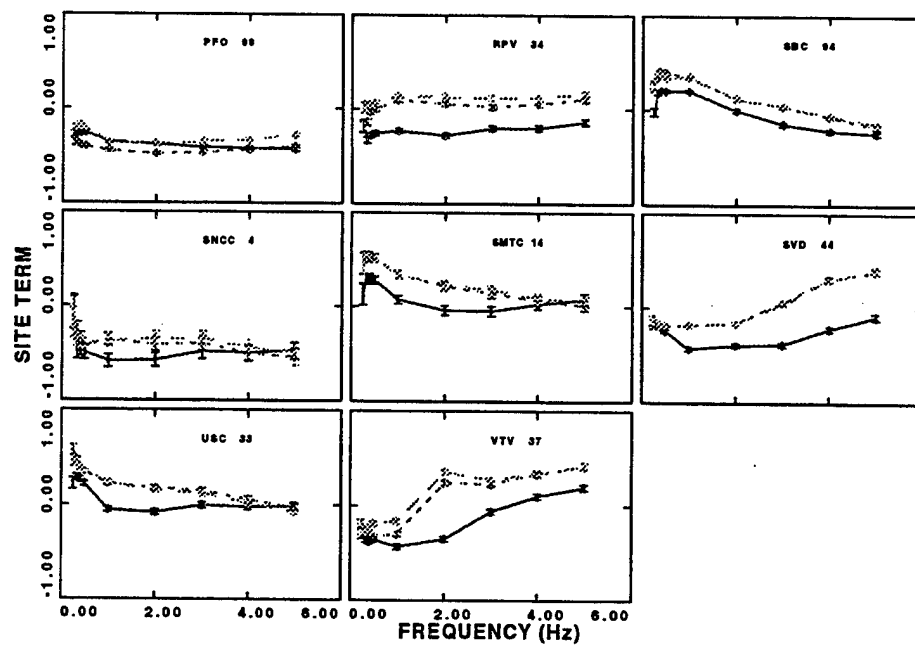


Fig. 14. Site terms for Fourier velocity spectra (cont'd).

Empirical H/Z Ratio TERRAscope Sites

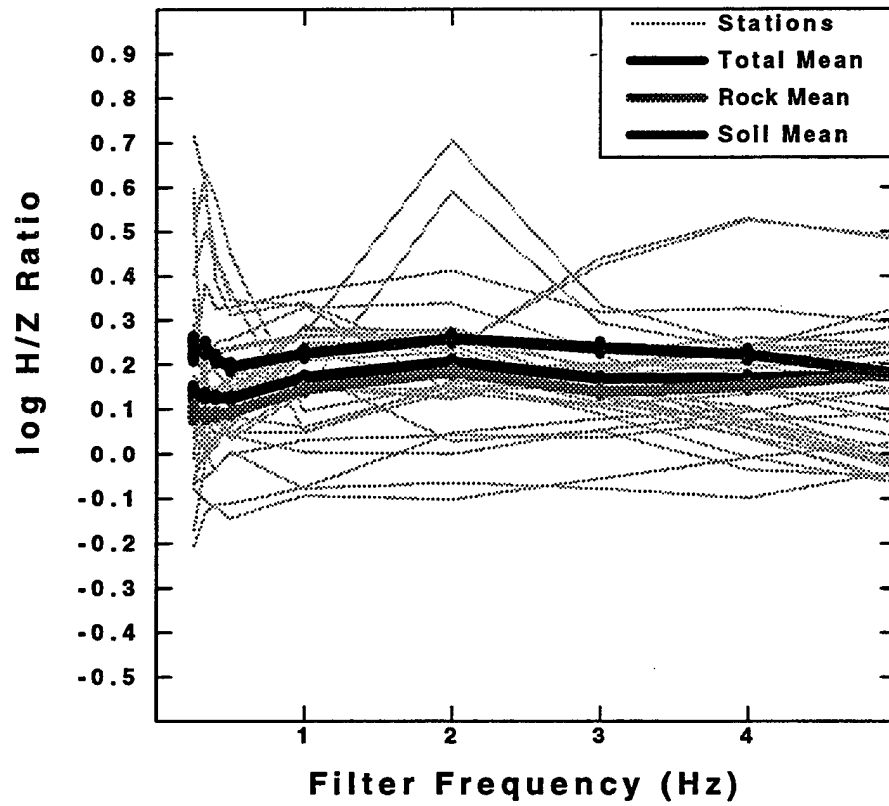


Fig. 15. Observed and mean H/Z ratio from the station terms of Figs 13 and 14.

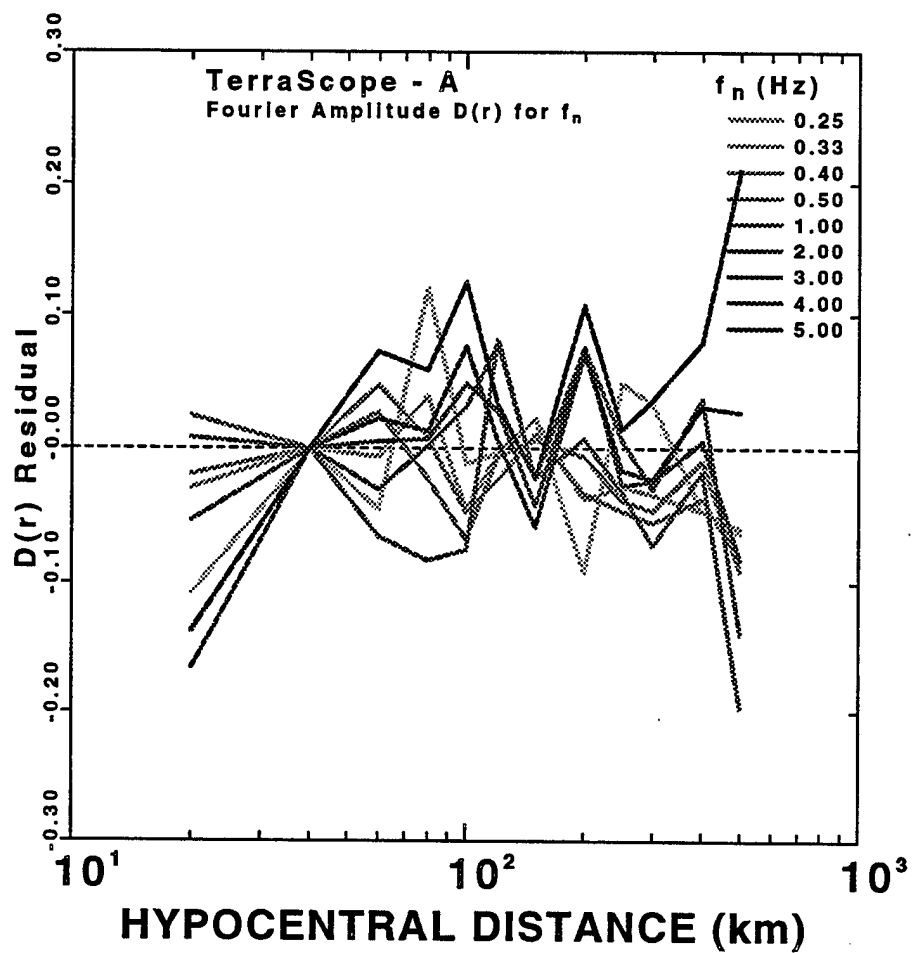


Fig. 16. Residuals of the model fit to the Fourier velocity distance function.

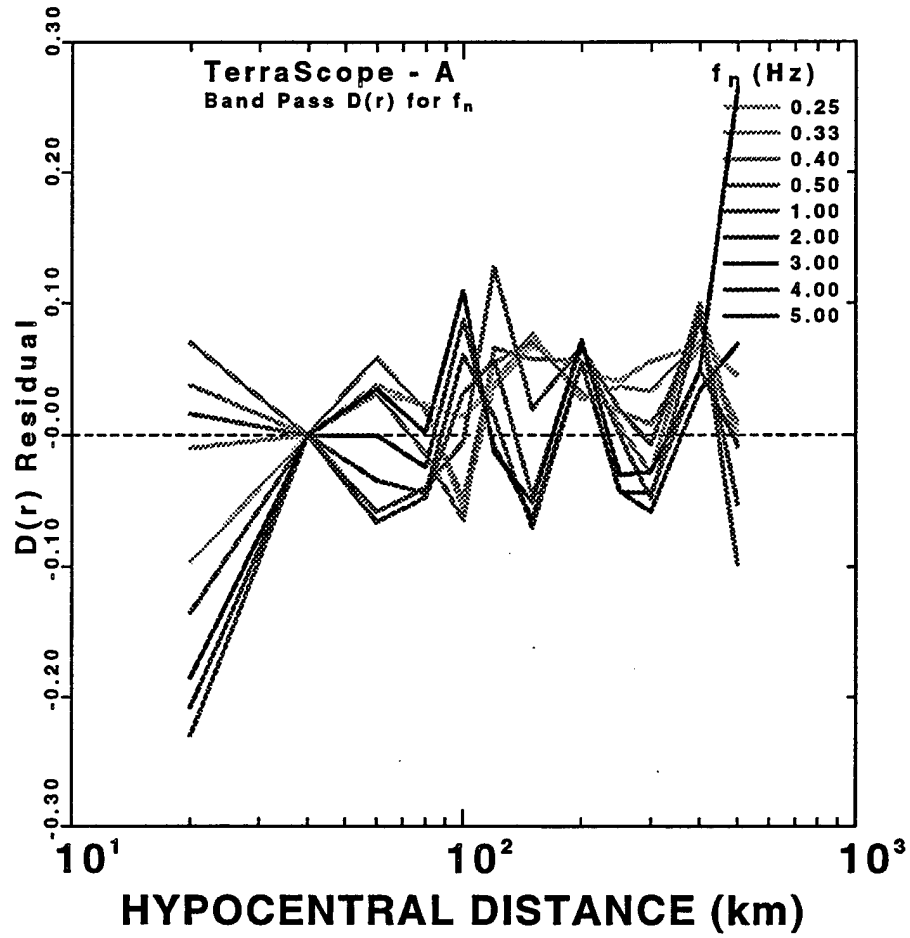


Fig. 17. Residuals of the model fit to the filtered time-domain velocity distance function.

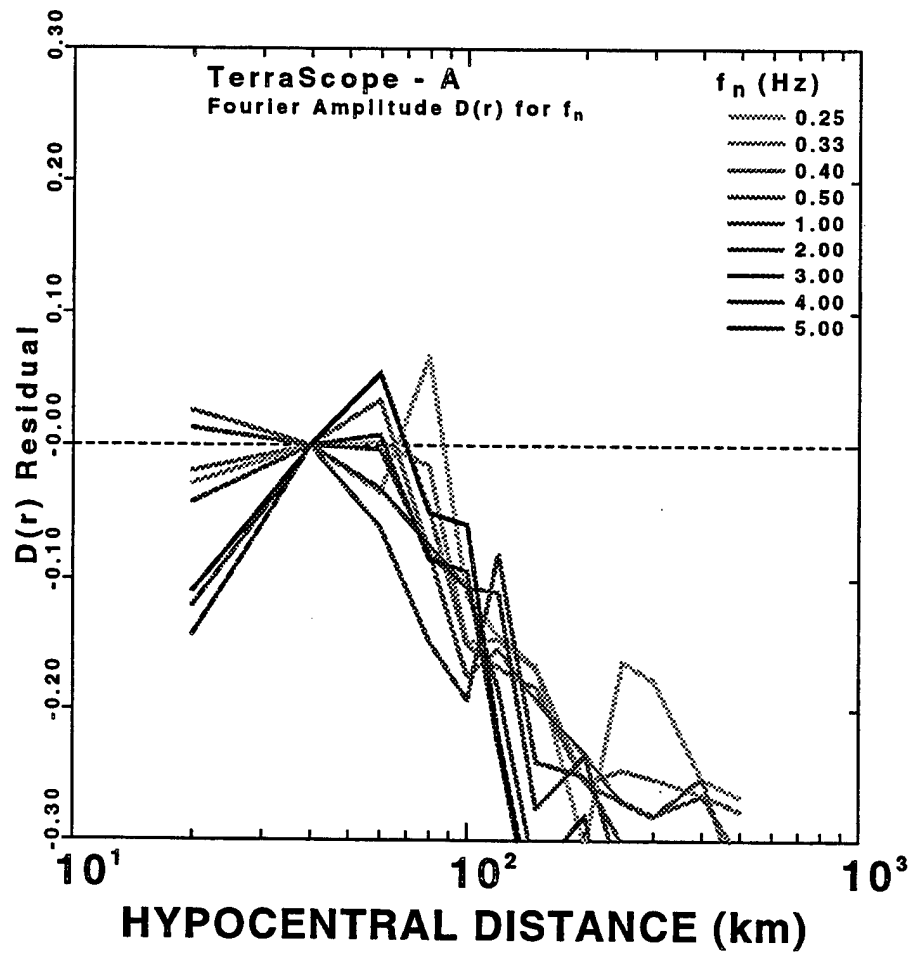


Fig. 18. Residuals of the model fit to the Fourier velocity distance function using the Atkinson and Silva (1997) $Q(f)$ and geometrical spreading function.

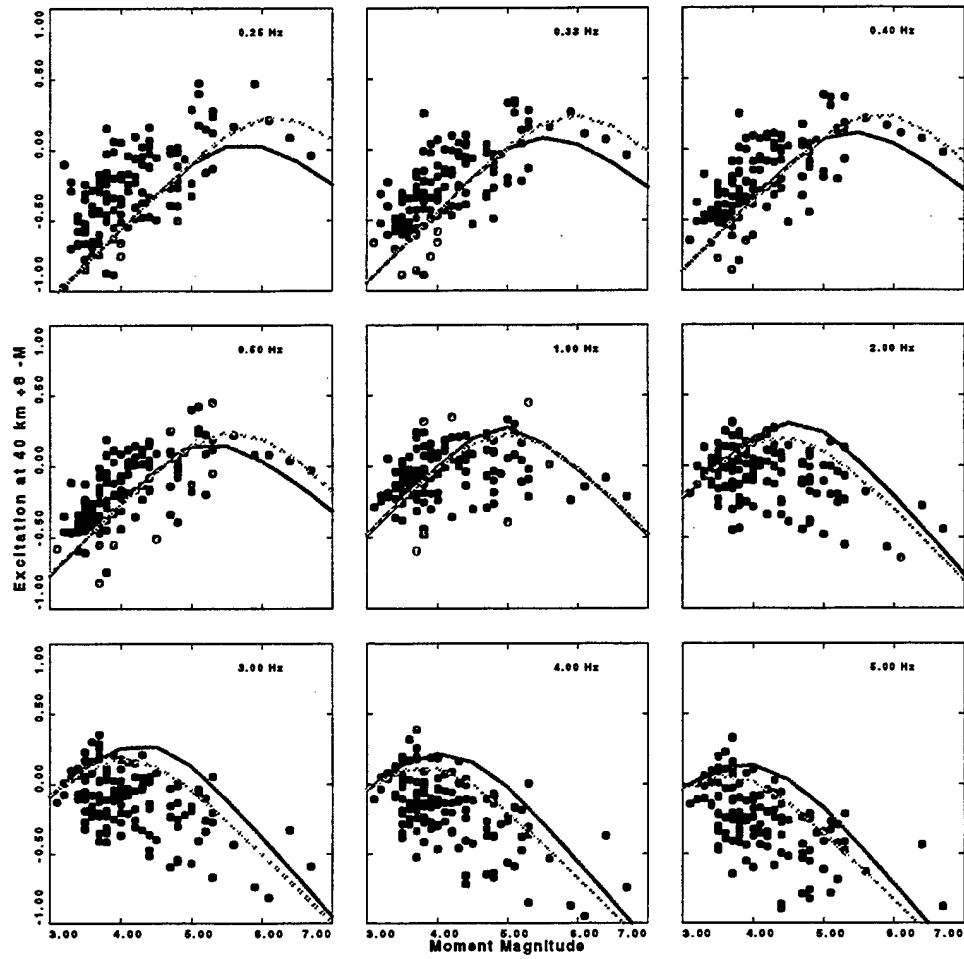


Fig. 19. Excitation of Fourier velocity spectra at 40 km. The solid curve is the prediction of the Atkinson and Boore (1998) source model; the dashed curve is that of the Boore and Joyner (1997) source model. E is the \log_{10} of the Fourier velocity spectra in m .

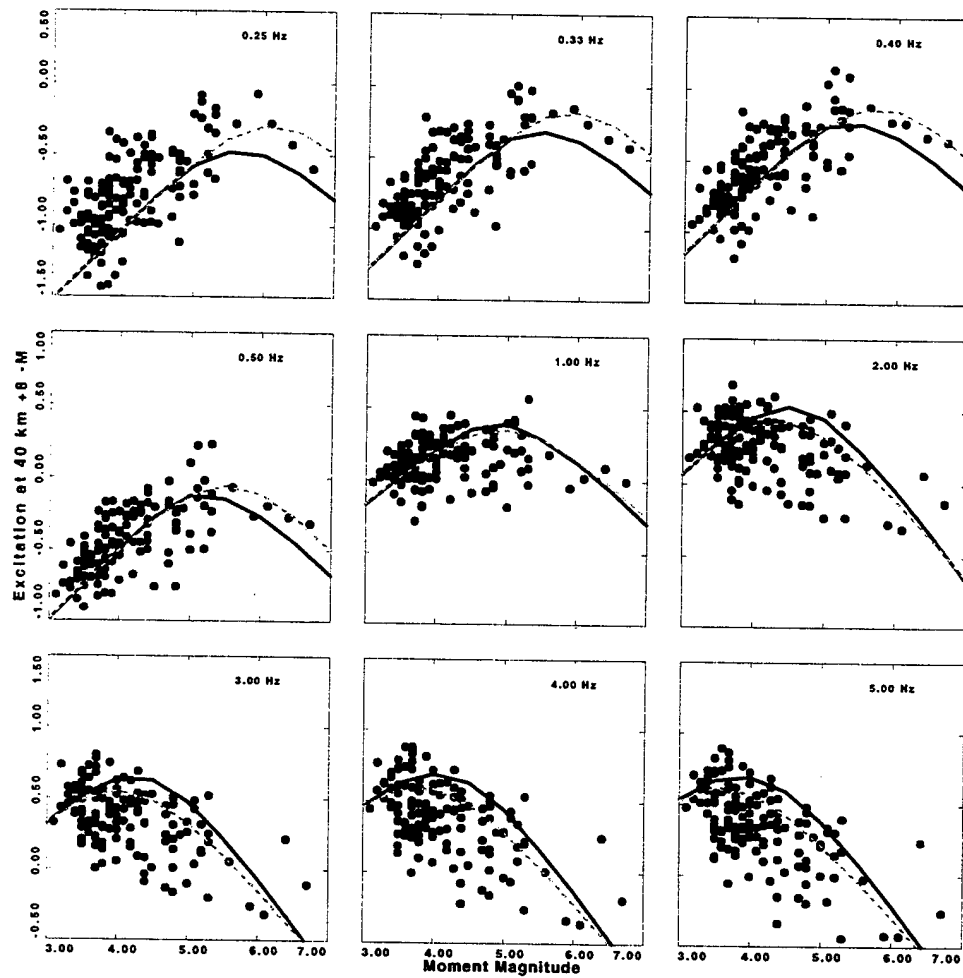


Fig. 20. Excitation of peak filtered time domain velocities at 40 km. The solid curve is the prediction of the Atkinson and Boore (1998) source model; the dashed curve is that of the Boore and Joyner (1997) source model. E is the \log_{10} of the filtered velocity spectra in m/sec .

THOMAS AHRENS
SEISMOLOGICAL LABORATORY 252-21
CALIFORNIA INST. OF TECHNOLOGY
PASADENA, CA 91125

AIR FORCE RESEARCH LABORATORY
ATTN: VSOP
29 RANDOLPH ROAD
HANSCOM AFB, MA 01731-3010 (2 COPIES)

AIR FORCE RESEARCH LABORATORY
ATTN: RESEARCH LIBRARY/TL
5 WRIGHT STREET
HANSCOM AFB, MA 01731-3004

AIR FORCE RESEARCH LABORATORY
ATTN: AFRL/SUL
3550 ABERDEEN AVE SE
KIRTLAND AFB, NM 87117-5776 (2 COPIES)

RALPH ALEWINE
NTPO
1901 N. MOORE STREET, SUITE 609
ARLINGTON, VA 22209

MUAWIA BARAZANGI
INSTOC
3126 SNEE HALL
CORNELL UNIVERSITY
ITHACA, NY 14853

DOUGLAS BAUMGARDT
ENSCO INC.
5400 PORT ROYAL ROAD
SPRINGFIELD, VA 22151

THERON J. BENNETT
MAXWELL TECHNOLOGIES
11800 SUNRISE VALLEY
SUITE 1212
RESTON, VA 22091

WILLIAM BENSON
NAS/COS
ROOM HA372
2001 WISCONSIN AVE. NW
WASHINGTON DC 20007

JONATHAN BERGER
UNIV. OF CALIFORNIA, SAN DIEGO
SCRIPPS INST. OF OCEANOGRAPHY IGPP, 0225
9500 GILMAN DRIVE
LA JOLLA, CA 92093-0225

ROBERT BLANDFORD
AFTAC
1300 N. 17TH STREET
SUITE 1450
ARLINGTON, VA 22209-2308

LESLIE A. CASEY
DEPT. OF ENERGY/NN-20
1000 INDEPENDENCE AVE. SW
WASHINGTON DC 20585-0420

CENTER FOR MONITORING RESEARCH
ATTN: LIBRARIAN
1300 N. 17th STREET, SUITE 1450
ARLINGTON, VA 22209

FRANCESCA CHAVEZ
LOS ALAMOS NATIONAL LAB
P.O. BOX 1663, MS-D460
LOS ALAMOS, NM 87545 (5 COPIES)

ANTON DAINTY
DTRA/PMA
45045 AVIATION DRIVE
DULLESVA 20166-7517

CATHERINE DE GROOT-HEDLIN
UNIV. OF CALIFORNIA, SAN DIEGO
IGPP
8604 LA JOLLA SHORES DRIVE
SAN DIEGO, CA 92093

DIANE DOSER
DEPT. OF GEOLOGICAL SCIENCES
THE UNIVERSITY OF TEXAS AT EL PASO
EL PASO, TX 79968

DTIC
8725 JOHN J. KINGMAN ROAD
FT BELVOIR, VA 22060-6218 (2 COPIES)

MARK D. FISK
MISSION RESEARCH CORPORATION
735 STATE STREET
P.O. DRAWER 719
SANTA BARBARA, CA 93102-0719

HENRY GRAY
SMU STATISTICS DEPARTMENT
P.O. BOX 750302
DALLAS, TX 75275-0302

I. N. GUPTA
MULTIMAX, INC.
1441 MCCORMICK DRIVE
LARGO, MD 20774

DAVID HARKRIDER
BOSTON COLLEGE
24 MARTHA'S PT. RD.
CONCORD, MA 01742

THOMAS HEARN
NEW MEXICO STATE UNIVERSITY
DEPARTMENT OF PHYSICS
LAS CRUCES, NM 88003

MICHAEL HEDLIN
UNIVERSITY OF CALIFORNIA, SAN DIEGO
SCRIPPS INST. OF OCEANOGRAPHY
9500 GILMAN DRIVE
LA JOLLA, CA 92093-0225

DONALD HELMBERGER
CALIFORNIA INST. OF TECHNOLOGY
DIV. OF GEOL. & PLANETARY SCIENCES
SEISMOLOGICAL LABORATORY
PASADENA, CA 91125

EUGENE HERRIN
SOUTHERN METHODIST UNIVERSITY
DEPT. OF GEOLOGICAL SCIENCES
DALLAS, TX 75275-0395

ROBERT HERRMANN
ST. LOUIS UNIVERSITY
DEPT. OF EARTH & ATMOS. SCIENCES
3507 LACLEDE AVENUE
ST. LOUIS, MO 63103

VINDELL HSU
HQ/AFTAC/TTR
1030 S. HIGHWAY A1A
PATRICK AFB, FL 32925-3002

RONG-SONG JIH
DTRA/PMA
45045 AVIATION DRIVE
DULLES, VA 20166-7517

THOMAS JORDAN
MASS. INST. OF TECHNOLOGY
BLDG 54-918
CAMBRIDGE, MA 02139

LAWRENCE LIVERMORE NAT'L LAB
ATTN: TECHNICAL STAFF (PLS ROUTE)
PO BOX 808, MS L-208
LIVERMORE, CA 94551

LAWRENCE LIVERMORE NAT'L LAB
ATTN: TECHNICAL STAFF (PLS ROUTE)
PO BOX 808, MS L-205
LIVERMORE, CA 94551

LAWRENCE LIVERMORE NAT'L LAB
ATTN: TECHNICAL STAFF (PLS ROUTE)
PO BOX 808, MS L-200
LIVERMORE, CA 94551

THORNE LAY
UNIV. OF CALIFORNIA, SANTA CRUZ
EARTH SCIENCES DEPARTMENT
EARTH & MARINE SCIENCE BUILDING
SANTA CRUZ, CA 95064

ANATOLI L. LEVSHIN
DEPARTMENT OF PHYSICS
UNIVERSITY OF COLORADO
CAMPUS BOX 390
BOULDER, CO 80309-0309

JAMES LEWKOWICZ
WESTON GEOPHYSICAL CORP.
325 WEST MAIN STREET
NORTHBORO, MA 01532

LOS ALAMOS NATIONAL LABORATORY
ATTN: TECHNICAL STAFF (PLS ROUTE)
PO BOX 1663, MS D460
LOS ALAMOS, NM 87545

LOS ALAMOS NATIONAL LABORATORY
ATTN: TECHNICAL STAFF (PLS ROUTE)
PO BOX 1663, MS F665
LOS ALAMOS, NM 87545

LOS ALAMOS NATIONAL LABORATORY
ATTN: TECHNICAL STAFF (PLS ROUTE)
PO BOX 1663, MS C335
LOS ALAMOS, NM 87545

GARY MCCARTOR
SOUTHERN METHODIST UNIVERSITY
DEPARTMENT OF PHYSICS
DALLAS, TX 75275-0395

KEITH MCLAUGHLIN
CENTER FOR MONITORING RESEARCH
SAIC
1300 N. 17TH STREET, SUITE 1450
ARLINGTON, VA 22209

BRIAN MITCHELL
DEPT OF EARTH & ATMOSPHERIC SCIENCES
ST. LOUIS UNIVERSITY
3507 LACLEDE AVENUE
ST. LOUIS, MO 63103

RICHARD MORROW
USACDA/IVI
320 21ST STREET, N.W.
WASHINGTON DC 20451

JOHN MURPHY
MAXWELL TECHNOLOGIES
11800 SUNRISE VALLEY DRIVE
SUITE 1212
RESTON, VA 22091

JAMES NI
NEW MEXICO STATE UNIVERSITY
DEPARTMENT OF PHYSICS
LAS CRUCES, NM 88003

ROBERT NORTH
CENTER FOR MONITORING RESEARCH
1300 N. 17th STREET, SUITE 1450
ARLINGTON, VA 22209

OFFICE OF THE SECRETARY OF DEFENSE
DDR&E
WASHINGTON DC 20330

JOHN ORCUTT
INST. OF GEOPH. & PLANETARY PHYSICS
UNIV. OF CALIFORNIA, SAN DIEGO
LA JOLLA, CA 92093

PACIFIC NORTHWEST NAT'L LAB
ATTN: TECHNICAL STAFF (PLS ROUTE)
PO BOX 999, MS K5-12
RICHLAND, WA 99352

FRANK PILOTTE
HQ AFTAC/TT
1030 S. HIGHWAY A1A
PATRICK AFB, FL 32925-3002

KEITH PRIESTLEY
DEPARTMENT OF EARTH SCIENCES
UNIVERSITY OF CAMBRIDGE
MADINGLEY RISE, MADINGLEY ROAD
CAMBRIDGE, CB3 0EZ UK

JAY PULLI
BBN SYSTEMS AND TECHNOLOGIES, INC.
1300 NORTH 17TH STREET
ROSSLYN, VA 22209

DELAINE REITER
WESTON GEOPHYSICAL CORP.
73 STANDISH ROAD
WATERTOWN, MA 0472

PAUL RICHARDS
COLUMBIA UNIVERSITY
LAMONT-DOHERTY EARTH OBSERV.
PALISADES, NY 10964

MICHAEL RITZWOLLER
DEPARTMENT OF PHYSICS
UNIVERSITY OF COLORADO
CAMPUS BOX 390
BOULDER, CO 80309-0309

DAVID RUSSELL
HQ AFTAC/TTR
1030 SOUTH HIGHWAY A1A
PATRICK AFB, FL 32925-3002

CHANDAN SAIKIA
WOODWARD-CLYDE FED. SERVICES
566 EL DORADO ST., SUITE 100
PASADENA, CA 91101-2560

SANDIA NATIONAL LABORATORY
ATTN: TECHNICAL STAFF (PLS ROUTE)
DEPT. 5704
MS 0979, PO BOX 5800
ALBUQUERQUE, NM 87185-0979

SANDIA NATIONAL LABORATORY
ATTN: TECHNICAL STAFF (PLS ROUTE)
DEPT. 9311
MS 1159, PO BOX 5800
ALBUQUERQUE, NM 87185-1159

SANDIA NATIONAL LABORATORY
ATTN: TECHNICAL STAFF (PLS ROUTE)
DEPT. 5736
MS 0655, PO BOX 5800
ALBUQUERQUE, NM 87185-0655

AVI SHAPIRA
SEISMOLOGY DIVISION
IPRG
P.O.B. 2286 NOLON 58122 ISRAEL

MATTHEW SIBOL
ENSCO, INC.
445 PINEDA CT.
MELBOURNE, FL 32940

JEFFRY STEVENS
MAXWELL TECHNOLOGIES
8888 BALBOA AVE.
SAN DIEGO, CA 92123-1506

TACTEC
BATTELLE MEMORIAL INSTITUTE
505 KING AVENUE
COLUMBUS, OH 43201 (FINAL REPORT)

LAWRENCE TURNBULL
ACIS
DCI/ACIS
WASHINGTON DC 20505

FRANK VERNON
UNIV. OF CALIFORNIA, SAN DIEGO
SCRIPPS INST. OF OCEANOGRAPHY
9500 GILMAN DRIVE
LA JOLLA, CA 92093-0225

RU SHAN WU
UNIV. OF CALIFORNIA, SANTA CRUZ
EARTH SCIENCES DEPT.
1156 HIGH STREET
SANTA CRUZ, CA 95064

JAMES E. ZOLLWEG
BOISE STATE UNIVERSITY
GEOSCIENCES DEPT.
1910 UNIVERSITY DRIVE
BOISE, ID 83725

SANDIA NATIONAL LABORATORY
ATTN: TECHNICAL STAFF (PLS ROUTE)
DEPT. 5704
MS 0655, PO BOX 5800
ALBUQUERQUE, NM 87185-0655

THOMAS SERENO JR.
SAIC
10260 CAMPUS POINT DRIVE
SAN DIEGO, CA 92121

ROBERT SHUMWAY
410 MRAK HALL
DIVISION OF STATISTICS
UNIVERSITY OF CALIFORNIA
DAVIS, CA 95616-8671

DAVID SIMPSON
IRIS
1200 NEW YORK AVE., NW
SUITE 800
WASHINGTON DC 20005

BRIAN SULLIVAN
BOSTON COLLEGE
INSITUTE FOR SPACE RESEARCH
140 COMMONWEALTH AVENUE
CHESTNUT HILL, MA 02167

NAFI TOKSOZ
EARTH RESOURCES LABORATORY
M.I.T.
42 CARLTON STREET, E34-440
CAMBRIDGE, MA 02142

GREG VAN DER VINK
IRIS
1200 NEW YORK AVE., NW
SUITE 800
WASHINGTON DC 20005

TERRY WALLACE
UNIVERSITY OF ARIZONA
DEPARTMENT OF GEOSCIENCES
BUILDING #77
TUCSON, AZ 85721

JIAKANG XIE
COLUMBIA UNIVERSITY
LAMONT DOHERTY EARTH OBSERV.
ROUTE 9W
PALISADES, NY 10964